Interannual changes of temperature and ozone: Relationship between the lower and upper stratosphere

Murry Salby, Patrick Callaghan, Philippe Keckhut, Sophie Godin, Marielle Guirlet

Interannual changes of temperature and ozone: Relationship between the lower and upper stratosphere

Murry Salby and Patrick Callaghan
Program in Atmospheric and Oceanic Sciences, University of Colorado, Boulder, Colorado, USA

Philippe Keckhut and Sophie Godin
Service d'Aeronomie/CNRS, Verrierre la Buisson, France

Marielle Guirlet
European Ozone Research Unit, University of Cambridge, Cambridge, England, United Kingdom

Received 1 February 2001; revised 23 August 2001; accepted 5 November 2001; published 17 September 2002.

[1] Changes of stratospheric dynamical structure and ozone are investigated in observations of the lower stratosphere, from meteorological analyses and Total Ozone Mapping Spectrometer (TOMS) ozone, and in contemporaneous observations of the upper stratosphere and mesosphere, from the French lidar at Observatoire de Haute-Provence (OHP). Interannual changes in the lower stratosphere are shown to be accompanied by coherent changes in the upper stratosphere and mesosphere. Over the 1980s and 1990s, both operate coherently with anomalous forcing of the residual mean circulation. Changes of temperature and ozone at OHP have sign and structure consistent with interannual changes of meridional transport. They reflect a poleward expansion and contraction of warm ozone-rich air, compensated by opposite changes of the polar-night vortex. *INDEX TERMS:* 3309 Meteorology and Atmospheric Dynamics: Climatology (1620); 3334 Meteorology and Atmospheric Dynamics: Middle atmosphere dynamics (0341, 0342); 0340 Atmospheric Composition and Structure: Middle atmosphere—composition and chemistry; *KEYWORDS:* ozone, temperature, stratosphere, interannual changes, Brewer-Dobson circulation

Citation: Salby, M., P. Callaghan, P. Keckhut, S. Godin, and M. Guirlet, Interannual changes of temperature and ozone: Relationship between the lower and upper stratosphere, *J. Geophys. Res.*, *107*(D18), 4342, doi:10.1029/2001JD000421, 2002.

1. Introduction

[2] The strength of wintertime stratospheric circulation is reflected in polar temperature, which undergoes large variations between years. So does total ozone at extratropical latitudes. Both are regulated by the residual mean circulation of the middle atmosphere. Air descending at high latitudes of the winter hemisphere experiences adiabatic warming that offsets radiative cooling, maintaining temperatures over the Arctic well above radiative equilibrium. Residual mean motion also transfers ozone poleward, its column abundance increasing steadily during winter until reaching its spring maximum.

[3] Interannual changes of dynamical structure in the lower stratosphere have been studied recently in global analyses from European Centre for Monthly Weather Forecasting (ECMWF) and related to contemporaneous changes of ozone observed by the Total Ozone Mapping Spectrometer (TOMS) [*Salby and Callaghan*, 2002, hereinafter referred to as SC]. Interannual changes of dynamical structure closely track anomalous forcing of the residual circulation, which varies between years with planetary wave driving and the quasi-biennial oscillation (QBO). Jointly, these mechanisms account for almost all of the observed variation of wintertime temperature in the lower stratosphere during the 1980s and 1990s. A similar relationship governs the interannual variation of ozone.

[4] The structure of interannual changes is consistent with changes of the residual circulation. During years when the residual circulation is intensified, temperatures over the Arctic are anomalously warm, reflecting enhanced downwelling and adiabatic warming that offsets longwave (LW) cooling inside polar darkness. This structure is visible well into the troposphere, sharing major features with the Arctic Oscillation [*Thompson and Wallace*, 1998]. During the same years, total ozone at extratropical latitudes is anomalously large, reflecting enhanced poleward transport of ozone-rich air from its photochemical source in the tropics. Just the reverse is observed during years when the residual circulation is weak. Accompanying changes at high latitudes are compensating changes at low latitudes, with which they operate coherently but out of phase. Both increase upward coherently to 10 mbar, the highest level represented in ECMWF analyses.

[5] Here, we investigate how interannual changes of dynamical and chemical structure in the lower stratosphere are related to behavior in the upper stratosphere and meso-

0148-0227/02/2001JD000421

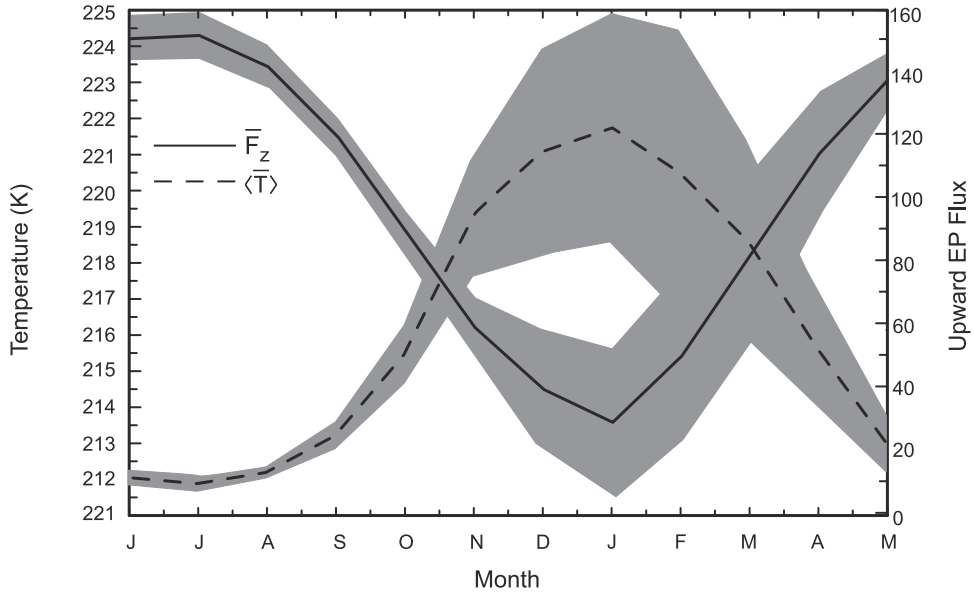

Figure 1. Mean annual cycle of column-averaged temperature above 100 mbar (solid) and normalized upward EP flux at 100 mbar (dashed), each averaged over 50N–90N, along with the standard deviation of their interannual variability (shaded).

sphere. Their relationship is explored in observations of temperature and ozone from the French lidar at Observatoire de Haute-Provence (OHP), which provides records above 30 km contemporaneous with those at lower levels from ECMWF and TOMS.

2. Data and Analysis

[6] Daily reanalyses from ECMWF provide global records of dynamical structure up to 10 mbar from 1979 to 1993. They have been continued through 1998 in ECMWF operational analyses and are supported by National Centers for Environmental Prediction (NCEP) reanalyses, which likewise span the 2 decades 1979–1998.

[7] The record of total ozone, which is concentrated below 10 mb, comes from the TOMS instrument. It operated on the Nimbus 7 satellite (1979–1993) and on the subsequent platforms Meteor-3 (1994) and Earth Probe (1997–1998).

[8] In the upper stratosphere and mesosphere, long records extending continuously over many years are rare. Addressing this shortcoming is the Network for the Detection of Stratospheric Change (NDSC), which began operation in 1991. At OHP (44N,6E), continuous monitoring of this region predates NDSC, with lidar measurements of temperature extending back to 1979.

[9] The lidar technique provides observations of temperature above 30 km with high vertical resolution and little dependence on calibration and instrumental changes. Temperature is deduced from Rayleigh scattering [*Hauchecorne and Chanin*, 1980], which yields good signal to noise between 30 and 80 km. These measurements yield a monthly mean record of temperature that is nearly continuous over the 1980s and 1990s. It lends itself well to studies of interannual variability, like the evaluation of trends [*Keckhut et al.*, 1995].

[10] Stratospheric ozone is also retrieved at OHP. From 1985 to 1993 the DIAL lidar observed ozone number density between 20 and 45 km [*Godin et al.*, 1989]. Since 1994, the technique has been modified to observe ozone between 12 and 45 km. These measurements of upper stratospheric ozone compare well with other techniques and have likewise been used to estimate trends [*Guirlet et al.*, 2000].

[11] The records of dynamical and chemical structure from the lower and upper stratosphere are reduced to monthly mean distributions. Quadratic quantities, like Eliassen-Palm (EP) flux, are first evaluated from daily values and then reduced to monthly means. From the monthly records we then calculate the wintertime decrease of temperature, which produces its minimum in January, and the wintertime increase of total ozone, which produces its maximum in spring. Each characterizes the annual cycle during individual years. Comparing values over the population of 20 years then determines interannual changes of temperature and ozone.

3. Annual and Interannual Variations of the Circulation

[12] The stratospheric circulation is characterized by column-averaged temperature between 100 and 10 mbar $\langle\overline{T}\rangle$, averaged over the Arctic, where $\langle\ \rangle$ denotes pressure-weighted column average and $\overline{(\ )}$ horizontal average between 50N and 90N reflects the strength of the wintertime vortex during individual years, which is related to how cold temperatures over the Arctic become. (Owing to pressure weighting, the column-average between 100 and 10 mbar nearly equals the column average extending upward indefinitely.) Figure 1 shows the mean annual cycle of $\langle\overline{T}\rangle$ (solid). Following summer solstice, $\langle\overline{T}\rangle$ decreases steadily until reaching a minimum in January. Its interannual variance (shaded) has similar seasonality, increasing sharply during the disturbed months of winter.

[13] Planetary wave activity transmitted upward from the troposphere has analogous seasonality. Superposed in Figure 1

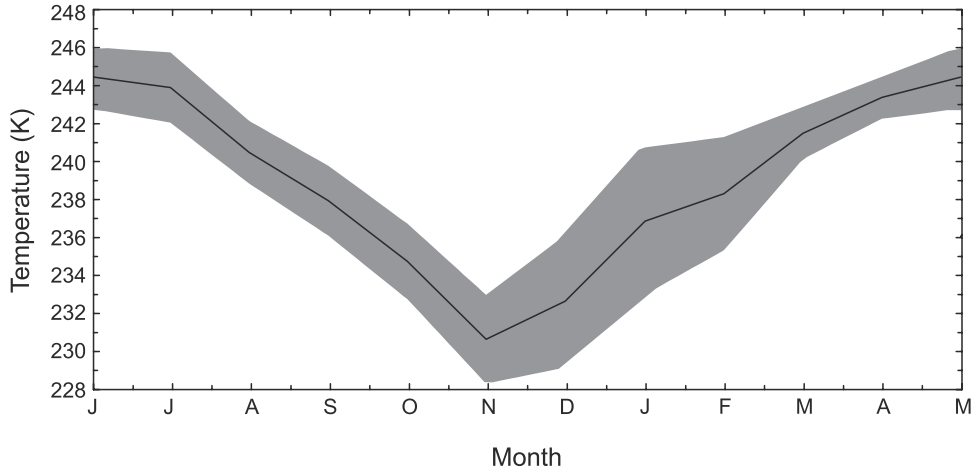

Figure 2. Mean annual cycle of column-averaged temperature above 30 km at Observatoire de Haute-Provence (OHP) (solid), along with the standard deviation of its interannual variability (shaded).

is the upward EP flux at 100 mbar $\overline{F}_z$ (dashed), averaged over the winter hemisphere between 50N and 90N. It measures momentum absorbed by the middle atmosphere, which drives the residual mean circulation. Westward drag exerted on the mean flow then leads, through the Coriolis force, to a poleward drift of air, which converges and sinks at high latitudes. $\overline{F}_z$ thus represents wave driving of the residual circulation and hence downwelling and adiabatic warming that accompany it.

[14] According to Figure 1, $\overline{F}_z$ has seasonality nearly opposite to $\langle \overline{T} \rangle$. Wave driving of the residual circulation maximizes shortly after winter solstice, when polar darkness leads to strong LW cooling over the Arctic. Radiative cooling is then offset by strong downwelling and adiabatic warming. The balance between these opposing influences controls the minimum temperature achieved around solstice during individual years. Simultaneously, the residual circulation transfers ozone-rich air poleward, thereby controlling the spring maximum of total ozone as well. The interannual variance of $\overline{F}_z$ (shaded) has similar seasonality. Largest changes are found during the dynamically disturbed season, when temperature changes are large.

[15] Temperature in the upper stratosphere has seasonality similar to that of of Arctic temperature in the lower stratosphere. Figure 2 plots the mean annual cycle of column-averaged temperature above 30 km at OHP (solid). Following summer solstice, $\langle T \rangle_{\mathrm{OHP}}$ decreases steadily until reaching a minimum shortly before winter solstice. Its interannual variance (shaded) likewise resembles the interannual variance of temperature in the lower stratosphere. Variance increases during the disturbed months of winter, although not as sharply as interannual variance over the Arctic (Figure 1).

[16] Temperature, ozone, and upward EP flux from the troposphere each experience sizable changes from one year to the next. For each variable these changes appear as deviations about the mean annual cycle. Over the 2 decades under consideration, they define a cloud of some 20 realizations of the annual cycle, characterized by the root-mean-square (RMS) variance in Figures 1 and 2 (shaded). An individual realization determines the interannual anomaly: the deviation from the 20-year mean annual variation. The analysis below explores how the anomaly during an individual year in the lower stratosphere is related to the anomaly during the same year in the upper stratosphere.

4. Interannual Changes of Dynamical Structure

[17] Interannual changes of Arctic temperature in the lower stratosphere are closely related to changes of planetary wave activity transmitted upward from the troposphere. Figure 3 plots, as a function of year, the anomalous wintertime decrease of column-averaged temperature over the Arctic during October–January (solid), $\Delta\langle \overline{T} \rangle^{\mathrm{Jan-Oct}}$. It's compared against the corresponding record of anomalous $\overline{F}_z$ (dashed), integrated over the same months. The latter represents the cumulative wave driving of the anomalous residual circulation during the months preceding the temperature minimum in January. It thus reflects anomalous downwelling and adiabatic warming during the winter season. Interannual changes in $\Delta\langle \overline{T} \rangle^{\mathrm{Jan-Oct}}$ closely track changes of westward momentum transmitted to the middle atmosphere by planetary waves. They also mirror changes of January temperature, which is determined almost entirely by changes during preceding months of the same winter (SC). The close relationship in Figure 3 isolates a major mechanism underlying the correspondence between planetary waves and polar temperature, identified in earlier analyses [*Labitzke*, 1981; *Baldwin and Dunkerton*, 1999; *Kodera et al.*, 2000]. With a correlation to observed changes of 0.92, anomalous forcing of the residual circulation accounts for almost all of the interannual variance of Arctic temperature.

[18] Interannual changes in the lower stratosphere are accompanied by changes in the upper stratosphere and mesosphere. Superposed in Figure 3 is the anomalous wintertime decrease of column-averaged temperature above 30 km observed at OHP, $\Delta\langle \overline{T} \rangle^{\mathrm{Jan-Oct}}$ (solid circles). These are local measurements, in contrast to the horizontally averaged behavior from ECMWF used to compute $\Delta\langle \overline{T} \rangle^{\mathrm{Jan-Oct}}$. As such, they are handicapped by additional variance that is incoherent on large scales but is filtered out from the horizontally averaged behavior considered in the

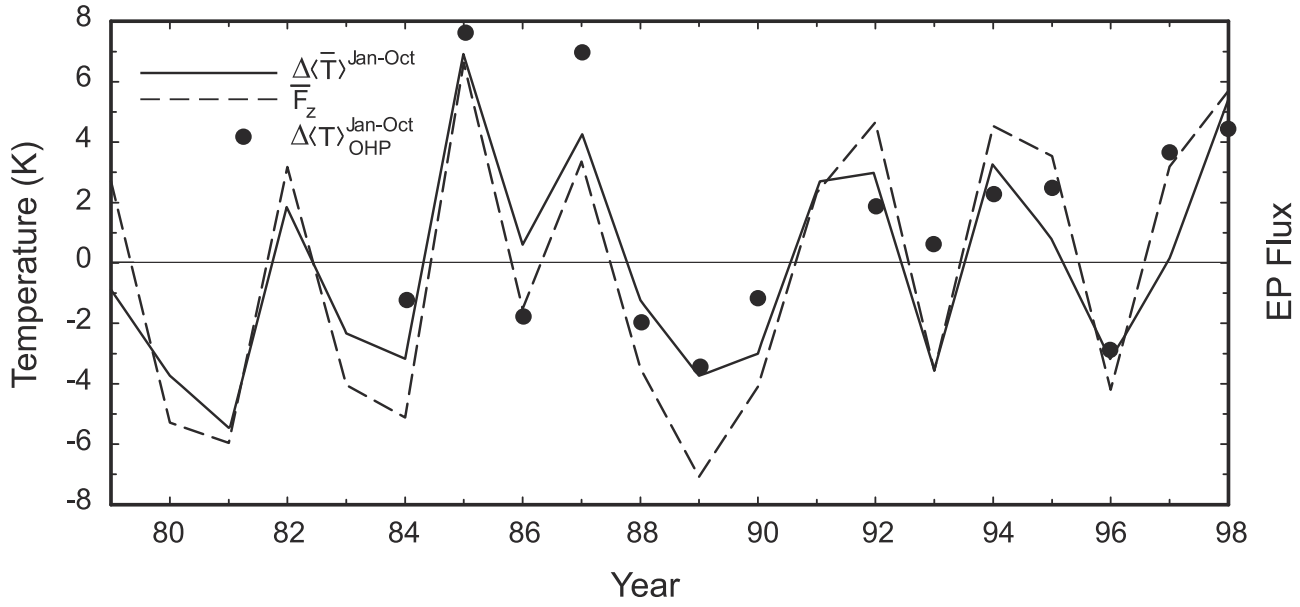

Figure 3. Anomalous wintertime decrease of column-averaged temperature above 100 mbar during October–January (60N – 90N), as a function of year, compared against the anomalous upward EP flux from the troposphere (50N–90N) integrated over the same months (normalized). Superposed is the anomalous wintertime decrease of column-averaged temperature above 30 km observed at OHP.

lower stratosphere. Some years are missing from the OHP record due to limited sampling by the lidar, observations from which are excluded by cloud cover. Note also that OHP, situated at 44N, lies south of the polar cap, over which $\Delta\langle\overline{T}\rangle^{\text{Jan-Oct}}$ has been averaged. Despite these limitations, the OHP record is strongly correlated to interannual changes of temperature in the lower stratosphere. In years when $\Delta\langle\overline{T}\rangle^{\text{Jan-Oct}}$ in the lower stratosphere is anomalously warm, so too is $\Delta\langle\overline{T}\rangle^{\text{Jan-Oct}}$ in the upper stratosphere. These are the same years when the residual circulation is intensified, implying enhanced adiabatic warming that offsets LW cooling. Just the reverse is observed in years when the residual circulation is anomalously weak. $\Delta\langle\overline{T}\rangle^{\text{Jan-Oct}}$ is then anomalously cold and so is $\Delta\langle\overline{T}\rangle^{\text{Jan-Oct}}$ in the upper stratosphere.

[19] The vertical structure of temperature changes has been composited against the record of anomalous $\overline{F}_z$. It follows from the local covariance between anomalous $\Delta\langle\overline{T}\rangle^{\text{Jan-Oct}}$ and $\overline{F}_z$ and then rescaling by their respective variances [see, e.g., Hendon and Salby, 1994]. The procedure constitutes a univariate regression that projects the record of anomalous temperature onto that of anomalous $\overline{F}_z$, which serves as the reference time series or "interannual clock." Resulting structure then describes temperature changes that operate coherently with anomalous forcing of the residual circulation.

[20] Figure 4 shows, as a function of altitude, the anomalous wintertime decrease of temperature at OHP (solid) introduced by a one standard deviation increase in forcing of the residual circulation. $\Delta\langle\overline{T}\rangle^{\text{Jan-Oct}}$ is 95% significant and positive from 30 to 60 km. It represents a wintertime decrease of temperature that is anomalously warm during years when the residual circulation is intensified. Below 10 mbar (Figure 3), $\Delta\langle\overline{T}\rangle^{\text{Jan-Oct}}$ likewise operates coherently with anomalous forcing of the residual circulation. Changes in the upper stratosphere in Figure 4 therefore operate coherently with interannual changes in the lower stratosphere. Above 60 km, temperature also changes coherently with temperature in the lower stratosphere. However, there, anomalous temperature reverses sign, varying out of phase with anomalous temperature below 60 km.

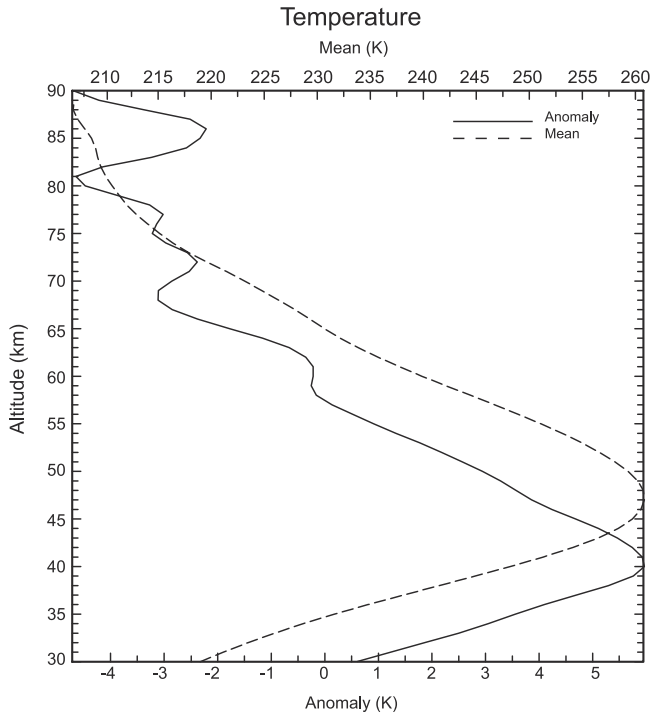

Figure 4. Anomalous wintertime decrease of temperature at OHP (solid), as a function of altitude, introduced by a one standard deviation increase in forcing of the residual circulation. Also shown is the 20-year mean temperature at OHP for October–January (dashed).

[21] The reversal of $\Delta\langle\overline{T}\rangle^{\mathrm{Jan-Oct}}$ coincides with the altitude where the meridional gradient of mean temperature reverses: Coldest temperatures are found over the winter pole in the stratosphere but over the summer pole in the mesosphere. The vertical structure of anomalous temperature, in fact, resembles mean thermal structure over OHP, which is superposed in Figure 4 (dashed). It too increases upward to ~45 km and then decreases in the mesosphere. The profile of anomalous temperature is displaced downward relative to mean temperature by ~5 km, reflecting downwelling that is also present.

[22] The similarity of temperature profiles in Figure 4, supported by the reversal of anomalous temperature above 60 km, suggests that much of the interannual change at OHP actually follows from changes of meridional transport. OHP is positioned equatorward of strong downwelling, which is concentrated poleward of 60N [see, e.g., *Garcia and Solomon*, 1983]. Residual motion is then dominated by poleward transport, from which changes of OHP temperature can be understood. Changes of $\overline{v}^*$ introduce a meridional swing of isotherms, especially in the upper stratosphere, where temperature decreases sharply toward the winter pole. During winters when the residual circulation is intensified, increased $\overline{v}^*$ along the sharp horizontal gradient displaces isotherms northward. Warm air south of OHP in the upper stratosphere then expands poleward. Simultaneously, the vortex recedes, shifting stratospheric temperatures at OHP to warmer values and introducing positive anomalous temperature above 60 km. In the mesosphere, however, the horizontal gradient is reversed: Temperature increases toward the winter pole. Cold air south of OHP then expands poleward, while the vortex recedes. This shifts temperatures at OHP to colder values, introducing negative anomalous temperature above 60 km. During winters when the residual circulation is weakened, just the reverse occurs.

5. Interannual Changes of Ozone

[23] The annual cycle of total ozone from TOMS (not shown) is lagged with respect to the annual cycle of temperature by 3 months, reflecting the time for ozone to be exported from its chemical source in the tropics to middle and high latitudes, where total ozone is concentrated.

[24] Analogous to temperature, its interannual variance is large during winter months leading up to its maximum, which is reached shortly after spring equinox. In addition, ozone has little memory from previous years [*Hadjinicolaou et al.*, 1997; *Fusco and Salby*, 1999a, 1999b], like temperature. Interannual changes in its spring maximum are determined almost entirely by changes in its wintertime increase during the preceding months.

[25] During late winter, when ozone increases, anomalous forcing of the residual circulation varies with $\overline{F}_z$ and also with the QBO, which controls where planetary wave activity is absorbed [e.g., *Tung and Yang*, 1994]. However, even then, changes of $\overline{F}_z$ account for most of the interannual variance. In some years these influences reinforce, whereas in others they oppose one another.

[26] Generalizing the univariate analysis of section 4 to a multivariate regression accounts for changes of both $\overline{F}_z$ and the QBO (SC). The covariance of anomalous temperature with anomalous forcing of the residual circulation is maximized for that phase of the QBO, which positions equatorial westerlies in the lowermost stratosphere and equatorial easterlies near 10 mbar. Since QBO phase descends with time, this is equivalent to representing it with equatorial wind at either level. Anomalous forcing of the residual circulation, inclusive of $\overline{F}_z$ and the QBO, then accounts for almost all of the interannual variance of temperature during late winter, as it does during early winter (Figure 1).

[27] A similar relationship holds for ozone. Figure 5 plots the anomalous wintertime increase of total ozone from TOMS $\Delta\langle\overline{\mathrm{O}}_3\rangle^{\mathrm{Mar-Nov}}$ during the months November–March (solid), averaged over the northern extratropics. Superposed is the anomalous ozone increase operating coherently with anomalous forcing of the residual circulation (dashed), integrated over the same season. Changes in the wintertime increase of TOMS ozone closely track anomalous forcing of the residual circulation. During years when the residual circulation is intensified, the wintertime increase of ozone is anomalously large. Just the reverse is observed during years when the residual circulation is weakened. It's noteworthy that this relationship holds even in years of unusually low ozone, like 1993 and 1997.

[28] Anomalous TOMS ozone in Figure 5 reflects interannual changes in the lower stratosphere, where total ozone is concentrated. Those changes are accompanied by interannual changes in the upper stratosphere. Superposed in Figure 5 is the anomalous wintertime increase of ozone column abundance above 30 km observed at OHP (solid circles). The OHP record is available during these months after 1986. It misses a couple of years, owing to limited sampling by the lidar. Nevertheless, the available data from the upper stratosphere are strongly correlated to fluctuations of TOMS ozone in the lower stratosphere, which in turn are strongly correlated to anomalous forcing of the residual circulation. (Because TOMS ozone is concentrated below 30 km, observations of it are virtually independent of observations of OHP column abundance above 30 km.) During years when forcing of the residual circulation is intensified, the wintertime increase of TOMS ozone is anomalously large and so is the wintertime increase of OHP ozone. During the same years, springtime temperature over the Arctic is anomalously warm. Just the reverse is observed during intervening years, when forcing of the residual circulation is weakened. The joint appearance of ozone changes in the lower and upper stratosphere characterizes interannual changes that are deep, operating coherently throughout the middle atmosphere.

[29] Figure 6 shows, as a function of altitude, the anomalous wintertime increase of ozone mixing ratio at OHP (solid) introduced by a one standard deviation increase in forcing of the residual circulation. Owing to the limited number of years available from the lidar, the vertical structure of $\Delta\langle\overline{\mathrm{O}}_3\rangle_{\mathrm{OHP}}^{\mathrm{Mar-Nov}}$ has been composited by grouping high and low years and then differencing the means of each group. Anomalous mixing ratio is positive at all altitudes. So is the equatorward gradient of mean ozone, in contrast to temperature, the meridional gradient of which reverses in the mesosphere.

[30] The structure of ozone changes above 30 km mirrors the mean structure of ozone mixing ratio during Novem-

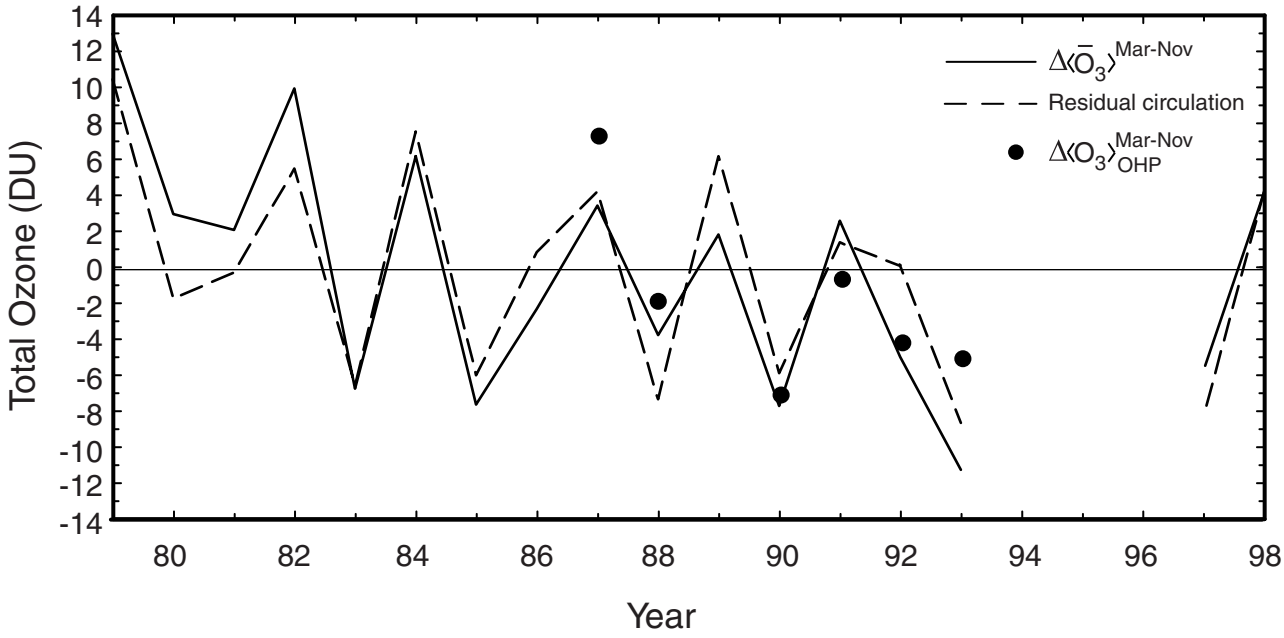

Figure 5. Anomalous wintertime increase of total ozone during November–March (10N–90N), as a function of year, compared against the anomalous residual circulation. Superposed is the anomalous wintertime increase of ozone column abundance above 30 km observed at OHP (renormalized).

ber–March, which is superposed in Figure 6 (dashed). Both peak near 30 km and decrease upward in very similar fashion. The resemblance of anomalous ozone to its mean, like temperature, is consistent with changes of meridional transport. Changes of $\bar{v}^*$ introduce a meridional swing of ozone mixing ratio surfaces. During winters when the residual circulation is intensified, increased $\bar{v}^*$ displaces mixing ratio surfaces northward. Ozone-rich air then expands poleward, while the vortex recedes. This is observed at OHP as a shift of the ozone profile to larger values, resulting in positive anomalous ozone at all altitudes. Conversely, during winters when the residual circulation is weakened, ozone-rich air experiences less poleward transport. It thus recedes equatorward, while the vortex expands. At OHP this is observed as a shift of the ozone profile to smaller values, resulting in negative anomalous ozone at all altitudes.

[31] The observed variation is consistent with the location of OHP measurements, which places them in the upper stratosphere and equatorward of strong downwelling. Residual motion is then dominated by poleward transport. Figure 7 presents mixing ratio surfaces from a three-dimensional (3-D) primitive equation model, inclusive of photochemistry [*Callaghan et al.*, 1999]. Two integrations are displayed: one forced by tropospheric planetary waves that are amplified, the other by tropospheric planetary waves that are weak. Under amplified conditions (dashed), mixing ratio surfaces in the upper stratosphere are displaced poleward of those resulting under weak conditions (solid). The difference, which marks intensified poleward transport, is especially noticable at high latitudes, where ozone is long-lived. In the lower stratosphere, where ozone behaves as a tracer throughout, mixing ratio surfaces at extratropical latitudes are displaced farther downward. They reflect an intensification of downwelling under amplified conditions.

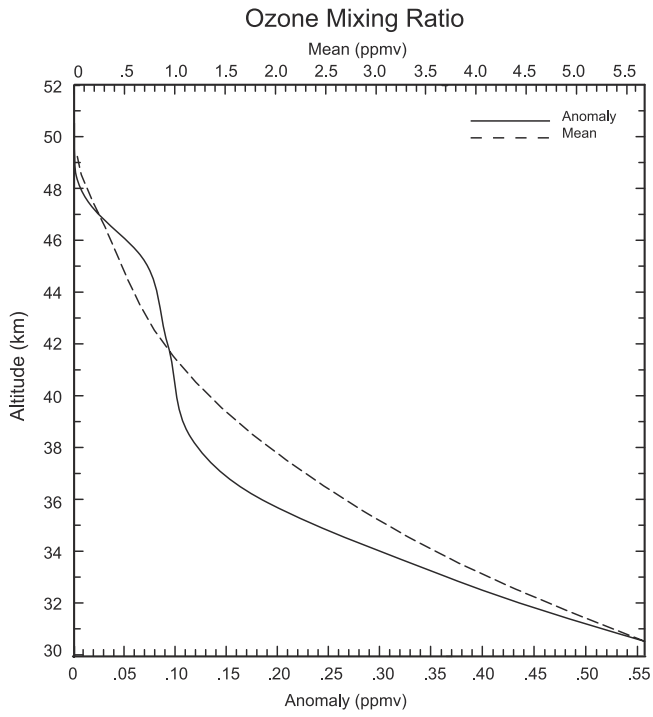

Figure 6. Anomalous wintertime increase of ozone mixing ratio at OHP (solid), as a function of altitude, introduced by a one standard deviation increase of the residual circulation. Composited by averaging anomalously high and low years. Also shown is the 20-year mean ozone mixing ratio at OHP for November–March (dashed).

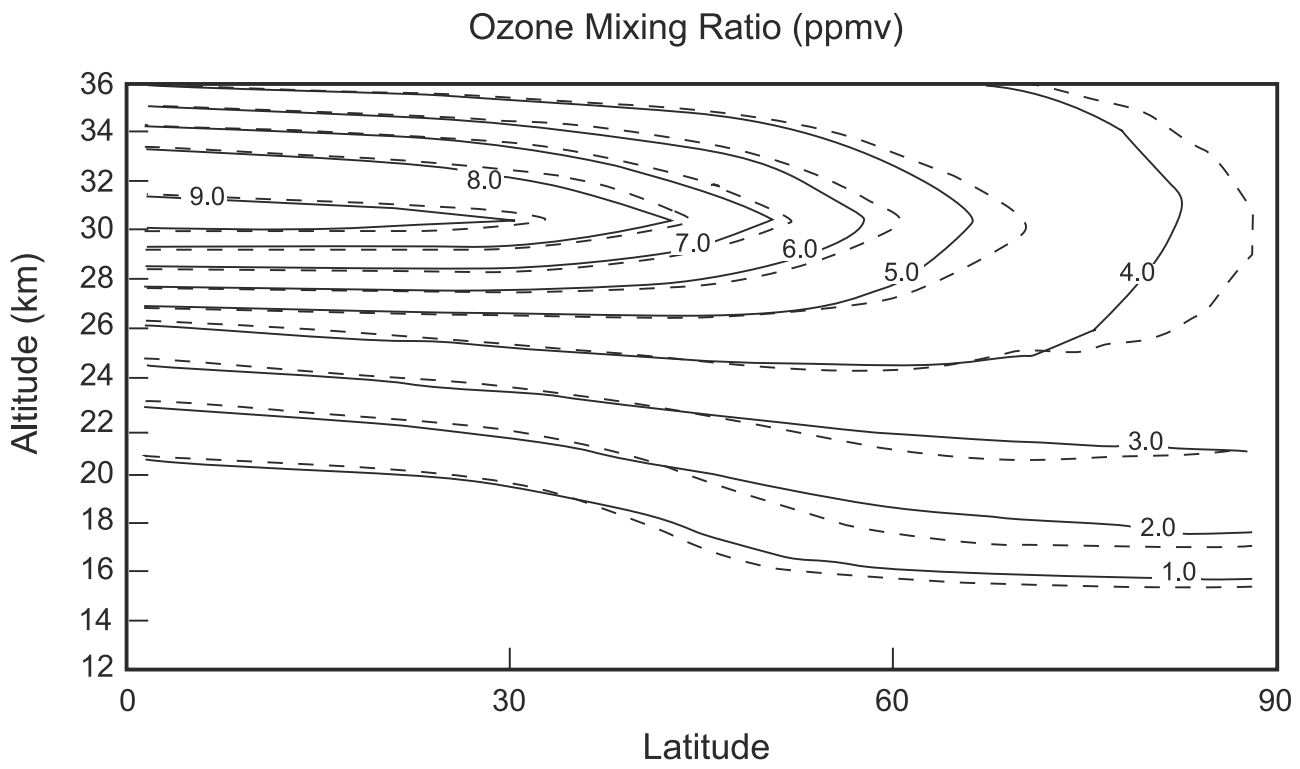

Figure 7. Zonal-mean ozone mixing ratio, as a function of latitude and altitude, from a 3-D primitive equation model forced by tropospheric planetary waves that are weak (solid) and amplified (dashed).

In the tropics, vertical displacements are reversed. They mark compensating changes and intensified upwelling. Those changes, however, are much smaller, mirroring upwelling that is an order of magnitude smaller than downwelling over the winter pole. Ozone changes in the tropics are also mediated by photochemistry, which offsets changes introduced through vertical transport and confines them to the lowermost stratosphere, where ozone is long-lived.

[32] In the region observed at OHP, ozone-rich air in Figure 7 expands poleward when the residual circulation is intensified. Simultaneously, the vortex recedes (not shown). Conversely, when the residual circulation is weakened, ozone-rich air recedes equatorward and, simultaneously, the vortex expands. Accomplished through changes of meridional transport, the latitudinal swing of mixing ratio surfaces displaces the ozone profile at midlatitudes between larger and smaller values. Ozone changes then resemble the mean vertical structure of ozone, which is displaced latitudinally.

6. Discussion

[33] Interannual changes of temperature and ozone in the upper stratosphere and mesosphere, observed at OHP, operate coherently with changes in the lower stratosphere. During years when values in the lower stratosphere increase, they simultaneously increase in the upper stratosphere. Changes in both regions operate coherently with anomalous forcing of the residual circulation, which varies with upward EP flux and the QBO.

[34] Interannual changes in the upper stratosphere at OHP are consistent with a northward expansion of warm ozone-rich air during winters when forcing of the residual circulation is intensified. Simultaneously, cold ozone-lean air inside the vortex recedes poleward. Just the reverse is observed during winters when forcing of the residual circulation is weakened.

[35] Changes observed at OHP, of course, represent only a single longitude. As such, they may also include zonally asymmetric changes, for example, displacements of the vortex from polar symmetry. Nonetheless, observed changes at OHP are consistent with zonal-mean changes at lower altitudes, where full coverage is available. They are also consistent with zonal-mean changes available in a 3-D model. Calculated changes there reflect changes of meridional transport, which follow from anomalous forcing of the residual circulation.

[36] Changes of the residual circulation also modify photochemistry, which can alter ozone as well. Intensified meridional transport carries air faster between radiative environments, driving it farther from local photochemical equilibrium. As a result, it alters ozone production inside air drifting poleward during the disturbed season. Such changes also influence chemical destruction. Winters when the residual circulation is weak lead to temperatures over the Arctic that are anomalously cold, as are observed during years of unusually low ozone. Accompanying reduced ozone transport, anomalously cold temperatures provide conditions favorable for heterogeneous processes, like those operating in the Antarctic lower stratosphere. Conversely, winters when the residual circulation is intensified lead to temperatures over the Arctic that are anomalously warm, inhibiting such processes.

[37] While heterogeneous chemistry can augment changes introduced directly by anomalous transport, it is

unlikely that it plays a central role in the observed changes of temperature and ozone. They operate coherently across much of the globe, changes at high latitudes being compensated at low latitudes by changes of opposite sign. Those interannual changes also have structure that is deep. As shown here, they extend upward coherently through the entire stratosphere.

[38] **Acknowledgments.** The authors gratefully acknowledge the support of Alain Hauchecorne and Marie-Lise Chanin, whose oversight of the OHP lidar for many years made this analysis possible. This work was performed while the lead authors were supported by NSF grant ATM-9732542.

References

Baldwin, M., and T. Dunkerton, Propagation of the Arctic Oscillation from the stratosphere into the troposphere, *J. Geophys. Res.*, *104*, 30,937–30,946, 1999.

Callaghan, P., A. Fusco, G. Francis, and M. Salby, A Hough spectral model for three-dimensional studies of the middle atmosphere, *J. Atmos. Sci.*, *56*, 1461–1480, 1999.

Fusco, A., and M. L. Salby, Interannual variations of total ozone and their relationship to variations of planetary wave activity, *J. Climate*, *12*, 1619, 1999a.

Fusco, A., and M. L. Salby, Interannual variations of total ozone and their relationship to variations of planetary wave activity: Corrigendum, *J. Climate*, *12*, 3165, 1999b.

Garcia, R., and S. Solomon, A numerical model of zonally-averaged dynamical and chemical structure of the middle atmosphere, *J. Geophys. Res.*, *88*, 1379, 1983.

Godin, S., G. Megie, and J. Pelon, Systematic lidar measurements of the stratospheric ozone vertical distribution, *Geophys. Res. Lett.*, *16*, 547–555, 1989.

Guirlet, M., P. Keckhut, S. Godin, and G. Megie, Description of the long-term ozone data series obtained from different instrumental techniques at a single location: The Observatoire de Haute-Provence (43.9N, 5.7E), *Ann. Geophys.*, *18*, 1325–1339, 2000.

Hadjinicolaou, P., J. Pyle, M. Chipperfield, and J. Kettleborough, Effect of interannual meteorological variability on middle latitude O_3, *Geophys. Res. Lett.*, *24*, 2993, 1997.

Hauchecorne, A., and M. L. Chanin, Density and temperature profiles obtained by lidar between 35 and 70 km, *Geophys. Res. Lett.*, *7*, 565–568, 1980.

Kodera, K., Y. Kuroda, and S. Pawson, Stratospheric sudden warmings and slowly propagating zonal-mean zonal wind anomalies, *J. Geophys. Res.*, *105*, 12,351–12,359, 2000.

Keckhut, P., A. Hauchecorne, and M. L. Chanin, Midlatitude long-term variability of the middle atmosphere: Trends and cyclic and episodic changes, *J. Geophys. Res.*, *100*, 18,887–18,897, 1995.

Labitzke, K., Stratospheric-mesospheric midwinter disturbances: A summary of observed characteristics, *J. Geophys. Res.*, *86*, 9665, 1981.

Salby, M., and P. Callaghan, Interannual changes of the stratospheric circulation: Relationship to tropospheric structure and ozone, *J. Clim.*, in press, 2002.

Thompson, D., and J. M. Wallace, The arctic oscillation signature in the wintertime geopotential height and temperature fields, *Geophys. Res. Lett.*, *25*, 1297, 1998.

Tung, K. K., and H. Yang, The influence of the equatorial quasi-biennial oscillation on the global circulation at 50 mb, *J. Atmos. Sci.*, *51*, 2708, 1994.

P. Callaghan and M. Salby, University of Colorado, Boulder, CO 80309, USA.

S. Godin and P. Keckhut, Service d'Aeronomie/CNRS, Verrierre la Buisson, BP3, 91371,Verrieres-le Buisson Cedex, France.

M. Guirlet, European Ozone Research Unit, University of Cambridge, Cambridge, CB2 1HE, United Kingdom.